Novel Fully Conjugated 2H- and Metal-Phthalocyanine Network Polymers: Synthesis, Characterization, and Dielectric Spectra Analysis

H. H. Abdel-Razik,[1]* K. H. Mahmoud[2†]

[1]*Chemistry Department, Faculty of Science, Taif University, Saudi Arabia*
[2]*Physics Department, Faculty of Science, Taif University, Saudi Arabia*

Received 19 July 2010; accepted 4 April 2011
DOI 10.1002/app.34608
Published online 15 August 2011 in Wiley Online Library (wileyonlinelibrary.com).

ABSTRACT: 2,7-*di*-*tert*-butylpyrene was oxidized to 2,7-*di*-*tert*-butylpyrene-4,5,9,10-tetraone. The latter through condensation reactions with vicinal diamine such as 4,5-diaminophthalonitrile produced heterocyclic monomer, 2,7-*di*-*tert*-butyl pyrene[4,5][9,10]bisquinoxaline-6,7-dinitrile, which was cyclo-tetramerized to the corresponding tetra[2,3-(1,4-diaza-6,6-*di*-*tert*-butylphenanthreno)[4,5]phthalocyanine]-based network polymer (2H-Pc), and tetra [2,3-(1,4-diaza-6,6-*di*-*tert*-butylphenanthreno)[4,5]phthalo-cyaninato metal II-based network polymers (M-Pc, M= Co, Ni, Zn, or Cu). Elemental analytical results, IR and NMR spectral data of the new prepared molecules are consistent with their assigned formulations. Molecular masses and metal contents of the synthesized polymers proved to be of high molecular masses which confirm the efficiency of tetramerization polymerization and complexation reactions. The dielectric constant (ε') and dielectric loss tangent (tan δ) were studied as a function of temperature and frequency. The detailed analysis of the results showed that the dielectric dispersion consists of both dipolar and interfacial polarization. Measurements of ac conductivity as a function of frequency at different temperatures revealed that the nonoverlapping small polaron tunneling is the most suitable mechanism for ac conduction behavior.
 J Appl Polym Sci 123: 1329–1339, 2012

Key words: phthalocynines; metallophthalocynines; dielectric constant; ac conductivity; correlated barrier hopping model

INTRODUCTION

The unique properties of phthalocyanines have generated worldwide interest in their use in many applications. Phthalocyanine (Pc) is a beautifully symmetrical 18 p-electron aromatic macrocycle, closely related to the naturally occuring porphyrins.[1] Owing to their increased stability, improved spectroscopic characteristics, diverse coordination properties, and architectural flexibility, phthalocyanines have surpassed porphyrins in a number of applications. Applications in organic solar cells[2,3] and transistors[4] are a natural function for these compounds. Light-emitting diodes in which phthalocyanines can be used as a hole transport layers[5,6] or emitting layers[7] were reported. Phthalocyanines are organic compounds able to act as chemically sensitive films[8,9] because of their capability of interaction with a large number of molecules. The synthetic route to new fully conjugated systems can be achieved through condensation of diones with diamines. For example, hexa-1, 5-diyne-3, 4-diones, react with diaminomaleodinitrile or 4,5-diaminophthalonitrile affording dicyanodiethynylpyrazines[10] or 2,3-dialkynylquinoxaline-6,7-dinitriles,[11] respectively.

Synthesis and characterization of the novel fully conjugated, tetrasubstituted H_2Pc containing four peripheral diimine binding sites, fused via pyrazine bridges to a metal free Pc core were reported.[12] Synthesis of highly soluble Pc from a new phthalonitrile under mild conditions was reported.[13] Cyclotetramerization of aromatic dinitriles with magnesium butoxide in refluxing butanol afforded tetrapyrazinoporphyrazines or tetra-6,7-quinoxalinoporphyrazines.[14] Derivatives of the new class of octaalkynyl tetra-[6,7]-quinoxalinoporphyrazines, analogues of the naphthalocyanines, were prepared in two steps starting from functionalized hexa-1,5-diyne-3,4-diones. Divalent zinc and magnesium ions were introduced into the macrocyclic core.[15] Condensation of diaminophthalonitrile with 1,10-phenanthroline-5,6-dione in ethanol afforded functionalized phthalonitrile precursor which was cyclotetramerized in a refluxing solution of lithium

**Present address:* Faculty of Science, Department of Chemistry, Mansoura University, New Damietta 34517, Egypt.
†*Present address:* Faculty of Science, Department of Physics, Cairo University, Cairo, Egypt.
Correspondence to: H. H. Abdel-Razik (hamada600@yahoo.co.uk).

metal dissolved in pentanol, followed by demetallation with acetic acid, affording the crude, metal free 2H-Pc as a dark green solid.[16] Microporous polymeric materials were prepared through double aromatic nucleophilic substitution reaction of appropriate hydroxylated aromatic monomers with 4,5-dichlorophthalonitrile yielding a bis(phthalonitrile) precursor that forms a Pc network, via a cyclotetramerization by a metal ion template.[17,18] A highly conducting macrocycle-linked metallophthalocyanine polymer was reported.[19] One of the methods to characterize materials is based on the analysis of their dielectric spectra. Dielectric analysis provides the information about the motion of entities having an electric charge or an electric dipole moment, i.e., dipole reorientation, rotation of the main and segmental chains, and conductivity mechanisms.[20] In this work, a new approach based on the synthesis and characterization of the novel fully conjugated, Pc-based network polymers for ac conductivity is introduced.

EXPERIMENTAL

Characterization

Fourier-transform infrared spectrometer (8101 M-Shimadzu) was used in spectral measurements. UV-vis spectra were obtained using Unicam UV-Vis spectrometer. NMR spectra were recorded in deuteriochloroform, on a Varian VXR 400S NMR spectrometer operating at 400 MHz (^{1}H NMR) and 100 MHz (^{13}C NMR) with tetramethylsilane as internal standards. Elemental analysis for metal content was carried out by a Perkin–Elmer Analyst 300, AAS atomic absorption spectrometer. Molecular masses (number average M_n, weight average M_w) were determined by gel permeation chromatography, GPC, (Polymer Laboratories, PL-GPC 20) using polystyrene standards and dilute polymer solutions (10 mg/5 mL) in tetrahydrofuran (THF) at room temperature with the rate of 1 mL /min. Elemental analysis was determined with Perkin-Elmer 2400 CHN.

Preparation of samples

Polymeric films were prepared by pouring the solution on a cleaned optically glass plate. This glass plate was kept over a pool of mercury for perfect levelling, so as to ensure uniform thickness and the solution was allowed to evaporate at room temperature. Aluminium electrodes were deposited by vacuum evaporation at 10^{-6} Torr, along the length of the glass plates, at the width of 3 mm, onto both surfaces of the samples to form a sandwich - type specimen in a cross-sectional area of 2.5×10^{-5} m^2 and thickness of 76 μm for dielectric measurements. Measurements of dielectric constant (ε') dielectric loss tangent (tan δ) in the frequency range 10^2–10^6 Hz and a controlled temperature range from 303 to 423 K were carried out using a Solartron 1260 impedance gain/phase analyzer (Solartron Instruments, Allentown, PA). The ac conductivity σ_{ac} of the sample, was obtained using the relation ($\sigma_{ac} = \omega\ \varepsilon_o\ \varepsilon'$ tan δ). The accuracy of both έ and tan δ was about ±3%.

Preparation of 2, 7-*di-tert*-butylpyrene-4, 5, 9, 10-tetraone 2

Pyrene was purchased from Acros and used as received. Other materials were obtained from Aldrich and used as received. 2,7-*di-tert*-butylpyrene **1** was synthesized by using the reported procedure[21] in greater than 90% yield. Compound 2 was prepared as previously reported.[22] To a solution of 2,7-*di-tert*-butylpyrene **1** (10 mmol) in CH_2Cl_2 (40 mL) and CH_3CN (40 mL) were added $NaIO_4$ (17.5 g, 81.8 mmol), H_2O (50 mL) and $RuCl_3.xH_2O$ (0.25 g, 1.2 mmol). The dark brown suspension was heated at 30–40°C overnight. The reaction mixture was poured into 500 mL of water, and the organic phase was separated. The aqueous phase was extracted with CH_2Cl_2. The CH_2Cl_2 extracts were combined with the organic phase and washed with water to give a dark orange solution. The solvent was removed under reduced pressure to afford a dark orange solid. Column chromatography (CH_2Cl_2) gave pure product as bright orange crystals, mp > 350°C.[22]

Preparation of 2, 7-*di-tert*-butylpyrene [4, 5][9,10]bis(2,3-quinoxaline-6,7-dinitrile) 3

A solution of tetraone **2** (10 mg, 0.027 mmol) in acetic acid (50 mL) was treated with diaminophthalonitrile (8.54 mg, 0.054 mmol). The mixture was refluxed with stirring at room temperature for 2 h. The precipitate was filtered off and washed with acetic acid to give pale yellow solid. 16.83 mg, yield = 86 %; mp = 292°C. IR (KBr): ν cm^{-1}, 2228 (CN), 1509 (C=N), 1618 (C=C). ^{1}H NMR ($CDCl_3$): δ 8.45 (s, 4H, quinoxaline-H), 7.73 (s, phenyl-H), 1.49 (s, 18H); ^{13}C NMR ($CDCl_3$): 150.7 (C), 149.8 (C), 145.3 (C), 144.9 (C), 141.1 (C), 141.5 (C), 136.3 (C), 136.5 (C), 132.1 (C), 132.4 (C), 129.9 (C), 129.7 (C), 127.6 (C), 127.8 (C), 115.7 (CN), 35.3 (C), 33.4 (C). Anal. calcd. for $C_{40}H_{26}N_8$, C, 77.65; H, 4.24; N, 18.11. Found: C, 77.67; H, 4.25; N, 18.09.

Preparation of Pc-based network polymer (2H-Pc) 4

Lithium metal (20 mg, 2.8 mmol) was added to a refluxing solution of **3** (309.34 mg, 0.5 mmol) in pentanol (2 mL). The solution was heated at reflux for 18 h. On cooling, acetic acid (0.2 mL) was added to the reaction mixture and the crude product was collected by centrifugation. The green material

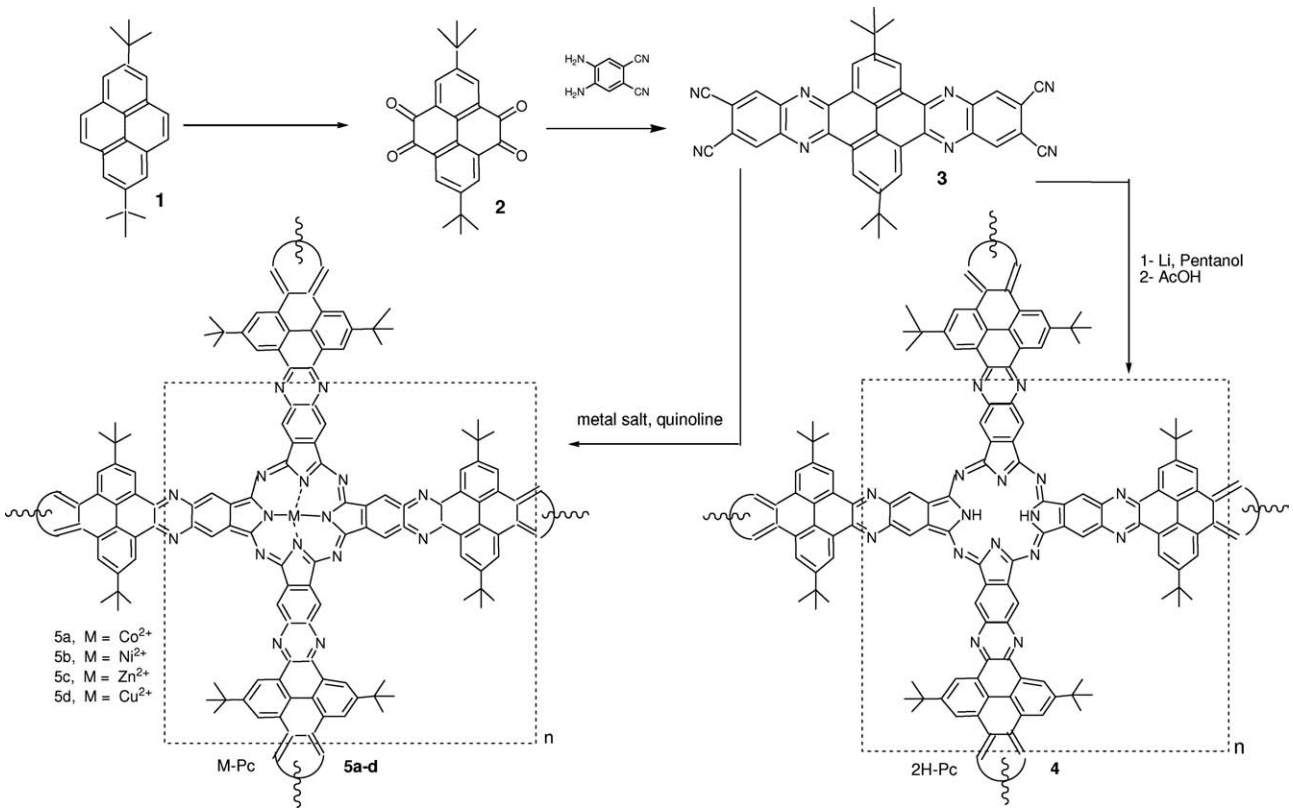

Scheme 1 Phthalocyanine network polymers derived from heterocyclic monomer.

was purified by column chromatography (eluent: dichloromethane) and by precipitation from toluene. IR (KBr): ν cm^{-1}, 1513 (C=N), 3350 (NH), 1604 (C=C). UV-Vis λ_{max} (CH_2Cl_2)/nm): 345, 652. ^1H NMR ($CDCl_3$) δ = 9.63 (s, 2H, NH); 7.73, 6.77 (s, aromatic-H), 1.55 (s, aliphatic-H)).

Preparation of phthalocyaninato metal II-based network polymer metal-phthalocyanine 5a-d

The monomer **3** (309.34 mg, 0.5 mmol) was subjected to form polymer networks **5a-b** on heating with 0.75 mmol of metal salt (cobalt II chloride, nickel II chloride, zinc acetate, or copper nitrate) and quinoline at 200°C. The material was dissolved in acetone, and the untrapped metal was precipitated and removed from the solution. To the resulting acetone solution, an excess of cold methanol was added, precipitating the green blue polymer. These polymers are blue (**5a, b**) or dark green (**5c, d**) solids. The solubility of these networks was examined in various solvents, showing that they are soluble in common organic solvents such as CH_2Cl_2, $CHCl_3$, THF and acetone at room temperature and are easily purified by chromatography on silica gel. The polymer was vacuum dried overnight.

- **5a**: IR (KBr): ν cm^{-1}, 1503 (C=N), 1608 (C=C). UV-Vis λ_{max} (CH_2Cl_2)/nm): 358, 665, 730 (shoulder). ^1H NMR ($CDCl_3$) δ = 7.69, 6.80 (s, aromatic-H), 1.59 (s, aliphatic-H)).
- **5b**: IR (KBr): ν cm^{-1}, 1508 (C=N), 1612 (C=C). UV-Vis λ_{max} (CH_2Cl_2)/nm): 355, 645, 710 (shoulder). ^1H NMR ($CDCl_3$) δ = 7.67, 6.78 (s, aromatic-H), 1.57 (s, aliphatic-H)).
- **5c**: IR (KBr): ν cm^{-1}, 1506 (C=N), 1618 (C=C). UV-Vis λ_{max} (CH_2Cl_2)/nm): 353, 655, 704 (shoulder). ^1H NMR ($CDCl_3$) δ = 7.71, 6.82 (s, aromatic-H), 1.54 (s, aliphatic-H)).
- **5d**: IR (KBr): ν cm^{-1}, 1500 (C=N), 1610 (C=C). UV-Vis λ_{max} (CH_2Cl_2)/nm): 360, 650, 720 (shoulder). ^1H NMR ($CDCl_3$) δ = 7.65, 6.77 (s, aromatic-H), 1.61 (s, aliphatic-H)).

RESULTS AND DISCUSSIONS

We report here, Synthesis and characterization of the novel fully conjugated, network polymers of tetramerized metal free Pc 2H-Pc and metal-phthalocyanine (M-Pc) containing four peripheral diimine binding sites. The synthetic route to these network polymers is summarized in Scheme 1. The key intermediate in the synthesis is the precursor 2, 7-*di-tert*-butylpyrene [4,5][9,10]bisquinoxaline-6,7-dinitrile **3**. The starting material is pyrene **1** which was synthesized by using the reported procedure[21] and was converted in the first step to 2,7-*di-tert*-butylPyrene-

4,5,9,10-tetraone **2,**[22] by treatment with $NaIO_4$ and $RuCl_3.xH_2O$. Condensation of **2** with commercially available 4,5-diaminophthalonitrile in acetic acid afforded the suitably functionalized 2,7-*di-tert*-butylpyrene[4,5][9,10]bisquinoxaline-6,7-dinitrile **3**, as a pale yellow solid. Cyclotetramerization of the aromatic tetranitrile **3** with lithium metal in pentanol and metal salt in quinoline generates Pc-based network polymer (2H-Pc) **4** and phthalocyaninato metal-based network polymers (M-Pc) **5a-d**, respectively.

The periphery of Pc macrocycles can be diversified by substituting with various substituent groups, which allow for enhanced solubility in most organic solvents and an alteration of the electronic properties of the Pc ring.[23] The presence of *tert*-butyl groups within the backbone of the prepared Pc network polymers has been shown to account for their greater solubility. These bulky *tert*-butyl groups along the two-dimensional polymer network backbone prevent an efficient packing of the macromolecules in the solid state generating sites of contortion. Microporosity within these organic polymer networks is attributed to their rigid and contorted structure.[17,18] Further structural modification by a change in the central metal atom can vary the excited state properties of the resultant M-Pc complexes.

Infrared and UV-Vis spectrum

The IR spectral data of precursor **3** show an intense bands at 2226, 1505, and 1614 cm^{-1} for C≡N, (C=N), and (C=C) groups, respectively. In accordance with this structure, the ^1H NMR spectrum revealed a singlet at $\delta = 8.45$, 7.73, and 1.49 assignable to aromatic and aliphatic protons. Elemental analytical results and ^{13}C NMR spectral data of the new tetranitrile **3** are consistent with the assigned formulation (see experimental, Scheme 1). IR spectrum of the free M-Pc network polymer 2H-Pc **4** shows a broad band at 1515 cm^{-1}, which is assignable to the stretching vibration of the C=N bond. The absorption values of the C=N vibration at 1504, 1507, 1505, and 1502 cm^{-1} for Co-Pc **5a**, Ni-Pc **5b**, Zn-Pc **5c**, and Cu-Pc **5d**, respectively, are lower by about 8–13 cm^{-1} than those for the metal free 2H-Pc **4**, which indicate the coordination of azomethine nitrogen atom to metal ions in the complexes.

UV-Vis spectrum of metal free Pc network polymer 2H-Pc **4** in dichloromethane solution shows a strong Soret band at 345 nm (Fig. 1). The Q band attributable to the difference between the highest occupied molecular orbital energy level and the lowest unoccupied molecular orbital energy, that is, the π-π* transitions in 2H-Pc **4** is observed at 650 nm. The electronic absorption spectra of the metal complexes **5a-d** in dichloromethane solution are dominated by two transitions (Fig. 2), namely the higher-energy B-band (broad band around 357 nm), and two characteristic lower-energy bands, Q-bands, around 655 nm and shoulder band around 720 nm, which can be assigned to the π-π* and/or d-π* transitions in the fused Pc ring structure.[24,25] The shoulder band is usually attributed to the 1s → 4d transition.[26] There is a little difference among the visible spectra of various M-Pc. Also, it has been suggested that both Q and B bands can be influenced by the metal-to-ligand charge-transfer bands.[27] It is clear that the absorption bands for metal complexes, extends beyond 800 nm (Fig. 2). Thus, these phthalocyanines could be useful in the field of optical data storage and for security printing, which require absorbance in the near infrared.

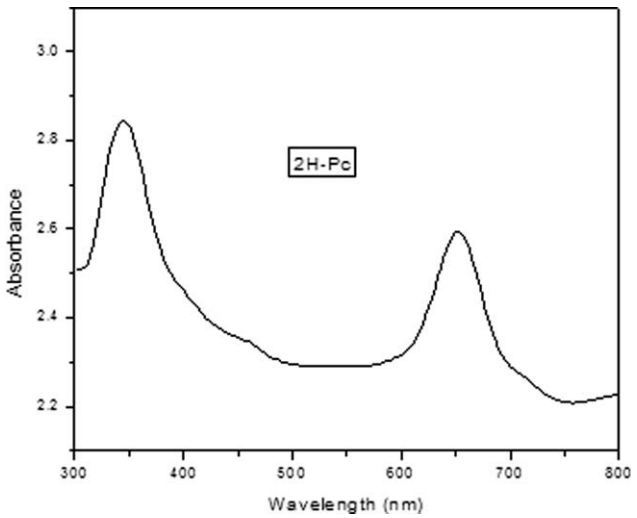

Figure 1 UV-Vis spectra of metal free-phthalocyanine (2H-Pc) 4.

^1H-NMR and molecular mass measurements of the prepared network polymers

^1H-NMR spectrum of metal free Pc network polymer 2H-Pc 4 reveals signals at $\delta = 7.73$, 6.77, and 1.55 assignable to aromatic and aliphatic protons. The presence of signal at $\delta = 9.63$ assignable to NH proton in 1H-NMR spectrum of 2H-Pc 4 gives direct evidence of the formation of an unsymmetrical tetradentate ligand. On the formation of metal complexes 5a-d, the signal of the NH groups disappear. All metal complexes show signals around $\delta = 7.68$, 6.78, and 1.57 assignable to aromatic and aliphatic protons, (see experimental, Scheme 1). Molecular masses and metal content of the synthesized polymers proved to be of high molecular masses, which confirm the efficiency of tetramerization polymerization and complexation reactions. The narrow molecular weight distribution (Table I) in all samples, with $M_w/M_n = 3.49$–4.40, implies that the polymerization follows a single-site reaction mechanism. The high

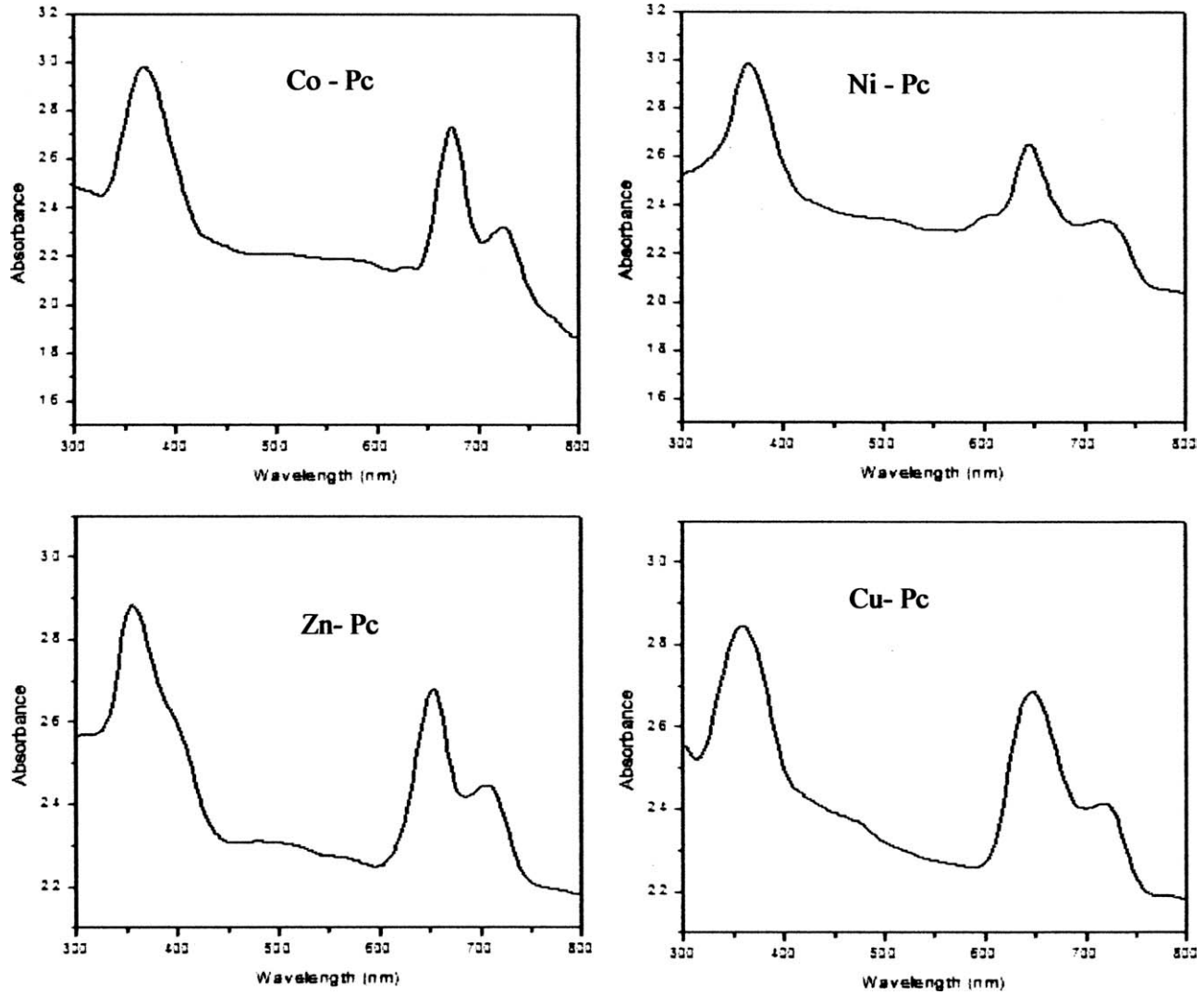

Figure 2 UV-Vis spectra of metal-phthalocyanines (M-Pc) 5a–d.

molar mass and good solubility of these polymers allow conventional solution-based polymer processing techniques.

These phthalocyanines have push–pull intramolecular charge-transfer chromophoric systems in which the pyrene and the pyrazine rings work as a donor group and an acceptor group, respectively. So these polymeric materials exhibit high electrical conductivity. The special conjugation in these phthalocyanines enables the electrons to delocalize throughout the whole system. In addition, the delocalized electrons may move around the whole network polymers to make them conductive. When electrons are removed from the backbone, resulting in cations or added to the backbone resulting in anions, the polymer can be transformed into a conducting form. Anions and cations act as charge carriers, hopping from one site to another under the influence of an electrical field, thus increasing conductivity. It is universally agreed that the doping process is an effective method to

TABLE I
Characteristic Data of the Prepared Phthalocyanine (Pc) Network Polymers

Samples	Yield (%)	Mp (°C)	Metal content wt (%)	M_n (g mol^{-1})	M_w (g mol^{-1})	Polydispersity (M_w/M_n)
2H-Pc	92	272–273	–	32282	133,754	4.14
Co-Pc	85	264–265	5.83	35,345	123,458	3.49
Ni- Pc	89	268–270	5.78	38,677	146,563	3,78
Zn- Pc	90	282–284	6.47	40,115	167,342	4.17
Cu- Pc	87	279–281	6.22	34,854	153,659	4.40

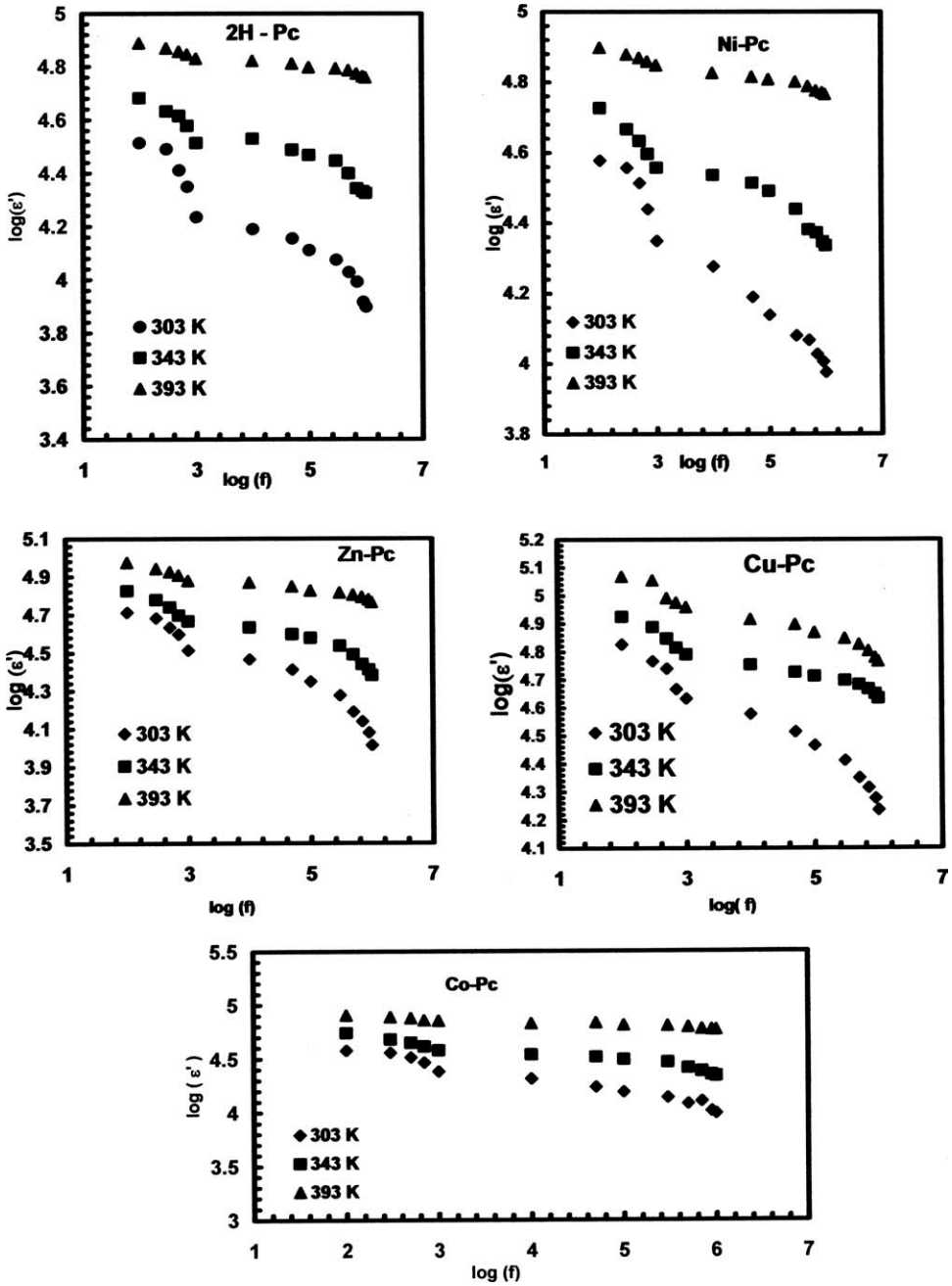

Figure 3 Frequency dependence of dielectric constant (ε′) of M-Pc at different temperatures.

produce conducting polymers as it allows electrons to flow through the conduction bands. As doping occurs, the electrons in the conjugated systems, which are loosely bound, are able to jump around the polymer chain.

Dielectric properties: Dielectric constant (ε′)

Dielectric relaxation studies are important to understand the nature and the origin of dielectric losses, which in turn, may be useful in the determination of the structure and defects in solids. The complex dielectric function is expressed as follows:[28,29]

$$\varepsilon^* = \varepsilon'(\omega) + i\varepsilon''(\omega) \quad (1)$$

where ε′ (ω) and ε′′ (ω) are the real and imaginary parts of the dielectric constant, respectively.

Figure 3 illustrates the variation of ε′ with frequency at different temperatures. It is clear that ε′ decreases with the increase of the applied frequency. This can be explained by means of dielectric polarization mechanism of the solid. Dielectric polarization occurs as electronic, ionic, interfacial, or dipolar polarization. Electronic and ionic polarizations are active in the high frequency range, whereas the other two mechanisms prevail in the low frequency

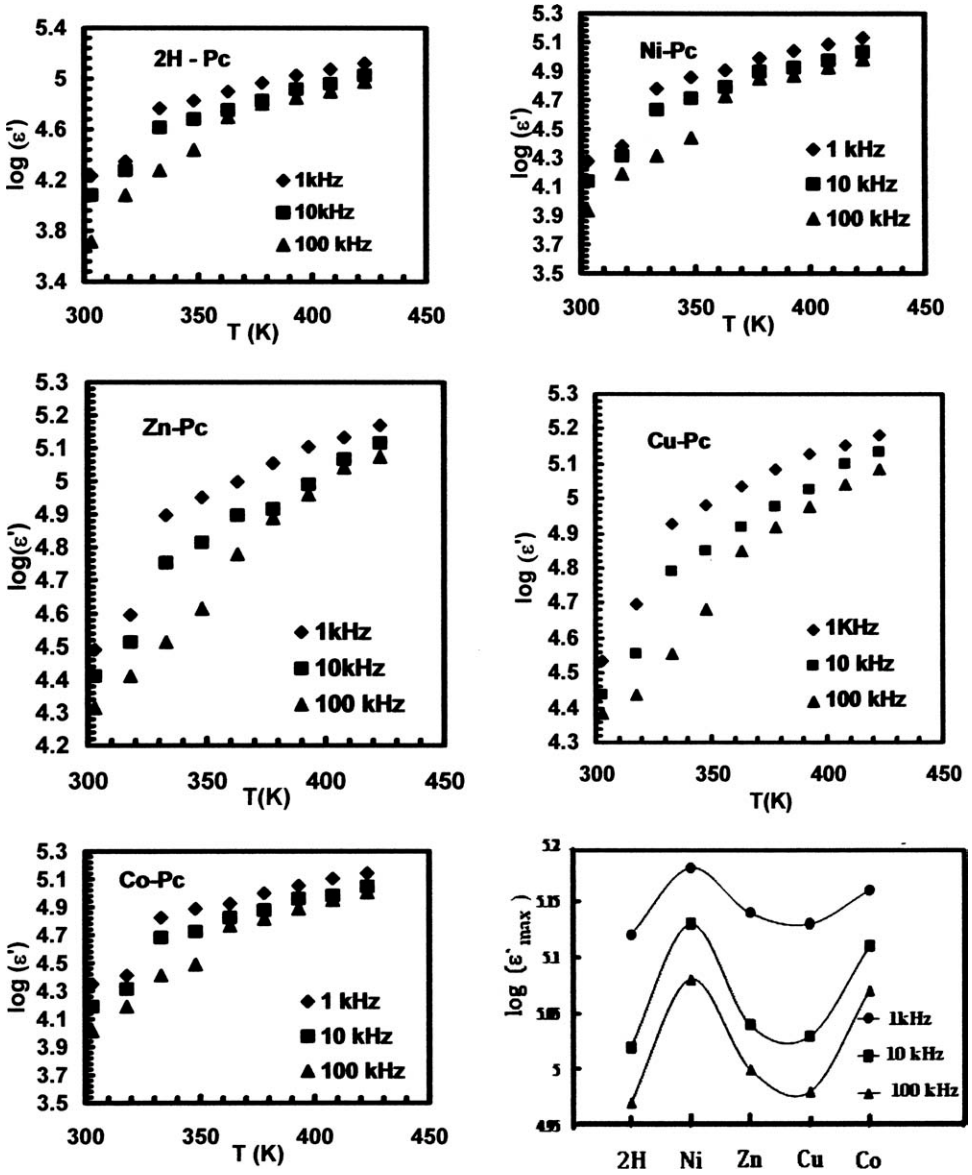

Figure 4 Temperature dependence of dielectric constant (ε′) of M-Pc at different frequencies; the last curve represents variation of maximum dielectric constant (ε'_{max}) for M-Pc samples.

range. The increase of ε′ toward the low frequency range may be attributed to interfacial polarization, which occurs via space charges formed in the material induce image charges on electrodes. In the presence of effective electrical field, these space charges which migrate are trapped by defects and a localized accumulation of charge is formed at the electrode and sample interfaces, consequently ε′ shows higher value at low frequencies.[30–32] The dielectric constant decreases with increasing the applied frequency. This effect is believed to be due to the screening of the electric field across the sample by charge redistribution.[33–35] At low frequencies, the charges on defects are more readily redistributed, such that defects closer to the positive side of the applied field become negatively charged, whereas the defects closer to the negative side of the field become positively charged. At different temperatures and as the frequency increases, the ε′ values become closer than in the case of lower frequencies. This can be attributed to the fact that the charges on the defects no longer have time to rearrange in response to the applied field. Figure 4 shows the temperature dependence of the dielectric constant ε′ at frequencies 1, 10, and 100 kHz for different M-Pc polymer samples. As shown in Figure 4 the dielectric constant decreases with increasing the frequency over the whole investigated range of temperatures. The increase of ε′ with temperature is governed mainly by the change in the intra- and inter-molecular interactions. These interactions may involve the alignment or rotation of the dipoles present in the

polymer with the increase of temperature.[36] It is noticed that there is no relaxation peak observed in the measured temperature range. The maximum dielectric constant (ε'_{max}) for M-Pc polymer samples is represented in Figure 4 (last curve). It is seen that Ni-Pc has the largest dielectric constant and this may be attributed to its lowest value of atomic volume, which yields larger free volume. The larger free volume will increase polarization as a result of facilitation of the molecular motion of polymer chain, which allows orientation of dipolar units.[37]

Dielectric loss tangent (tan δ)

The dielectric loss factor is the phase difference due to the loss of energy within the sample at a particular frequency and is expressed as tan δ ($\varepsilon''/\varepsilon'$). The dielectric loss is mainly attributed to thermally activated relaxation of freely rotating dipoles, where thermal energy is the only type of relaxation. Wheras at higher temperatures it is due to the electrical conduction with hopping motion of ions. The variation of dielectric loss with temperature is represented in Figure 5 for M-Pc polymer samples at 1 kHz. This relaxation can be considered dielectric relaxation. This can be confirmed through studying the variation of dielectric loss tangent as a function of frequency and this is represented in Figure 6. The tan δ (f) plots show asymmetric maxima at the dispersion region of ε' (ω). The maximum (tan δ (max) shifts to higher frequency with the increase of temperature suggesting that the effect of electrode polarization can be avoided. The peak frequency corresponding to tan δ (max) is known as relaxation frequency f_m. When $f < f_m$, the charge carriers are mobile over large distance and are associated with the hopping conductivity. On the other hand, when $f > f_m$ the carriers are spatially confined to their potential wells, mobile over short distances and associated with the relaxation polarization process.[38] Thus, the peak frequency f_m is indication of the transition from long range to short range mobility and is defined by the condition $2\pi f_m \tau_m = 1$, where τ_m is the relaxation time. The asymmetric tan δ (max) peak originates from the nature of relaxation behavior. This non-Debye behavior of the tan δ spectrum can be associated to the distribution of relaxation times. Having different environments, the contorted nature of samples and hence a distribution of mobile ion sites, is thought to be the cause for the non-Debye peak.

Ac conductivity (σ_{ac})

Figure 7 shows the frequency dependence of σ_{ac} (ω) at different temperatures for the M-Pc polymer samples. As can be seen, each curve displays the conductivity dispersion, which is strongly dependent on frequency

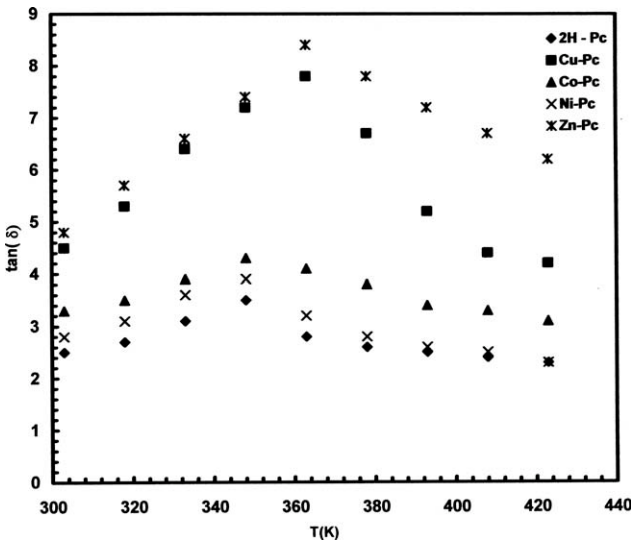

Figure 5 Variation of dielectric loss tangent (tan δ) with temperature for M-Pc at 1 kHz.

at room temperature and shows weaker frequency dependence at higher temperatures. Within the considered frequency and temperature ranges, the measured ac conductivity obeys a power law of the form[39]:

$$\sigma_{ac}(\omega) = A\omega^s \tag{2}$$

where A is temperature dependent pre-exponential factor, s power exponent.

The temperature dependence of the exponent (s) is calculated using plots of log σ_{ac} – log ω, in the considered temperature range and is shown in Figure 8. It is observed that (s) increases with increasing temperature. In literature, various models have been proposed to explain the behavior of the exponent (s) with solid materials,[39] and consequently the suitable operated conduction mechanism. In the simple quantum mechanical tunneling (QMT) model,[40] the exponent (s) can be calculated using the formula:

$$s = 1 - \frac{4}{\ln(\frac{1}{\omega\tau_o})} \tag{3}$$

where t_o is the characteristic relaxation time. In the QMT model, the frequency exponent (s) is temperature independent but frequency dependent.

A temperature and frequency dependent exponent can be obtained within the framework of the QMT model in the pair approximation by assuming that the carriers form nonoverlapping small polaron tunneling (NSPT)[40] where (s) in this case is given by:

$$s = 1 - \frac{4}{\ln(\frac{1}{\omega\tau_o}) - \frac{W_H}{kT}} \tag{4}$$

where W_H is the polaron binding energy.

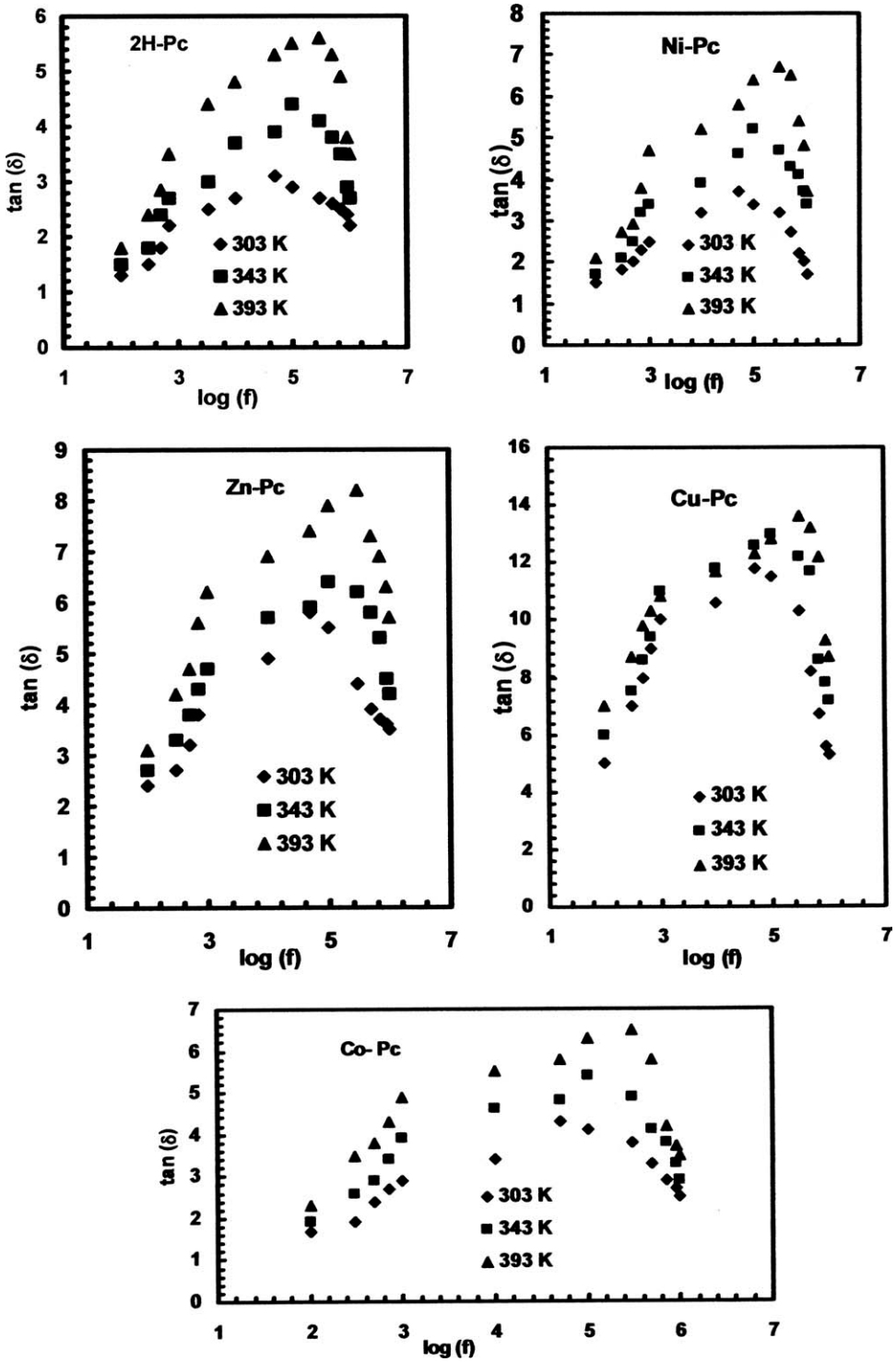

Figure 6 Variation of dielectric loss tangent (tan δ) with frequency for M-Pc at different temperatures.

That is, in the NSPT model s is temperature dependent which increases with the increase of temperature. A mechanism for the polaron tunneling, called the overlapping large polaron tunneling (OLPT) model is proposed by Long,[41] where the exponent s is given by:

$$s = 1 - \frac{8\alpha R_\omega + (6\beta W_{HO} r_p / R_\omega)}{(2\alpha R_\omega + \beta W_{HO} r_p / R_\omega)^2} \quad (5)$$

where $\beta = 1/kT$, α is the exponential decay parameter of the localized states wave function, R_ω is the hopping length at angular frequency ω, r_p is the polaron radius and W_{HO} depends on the effective dielectric constant of the material ε_p.[40,42]

Thus, the OLPT model predicts that the exponent (s) is both frequency and temperature dependent, besides its decrease from unity with increasing

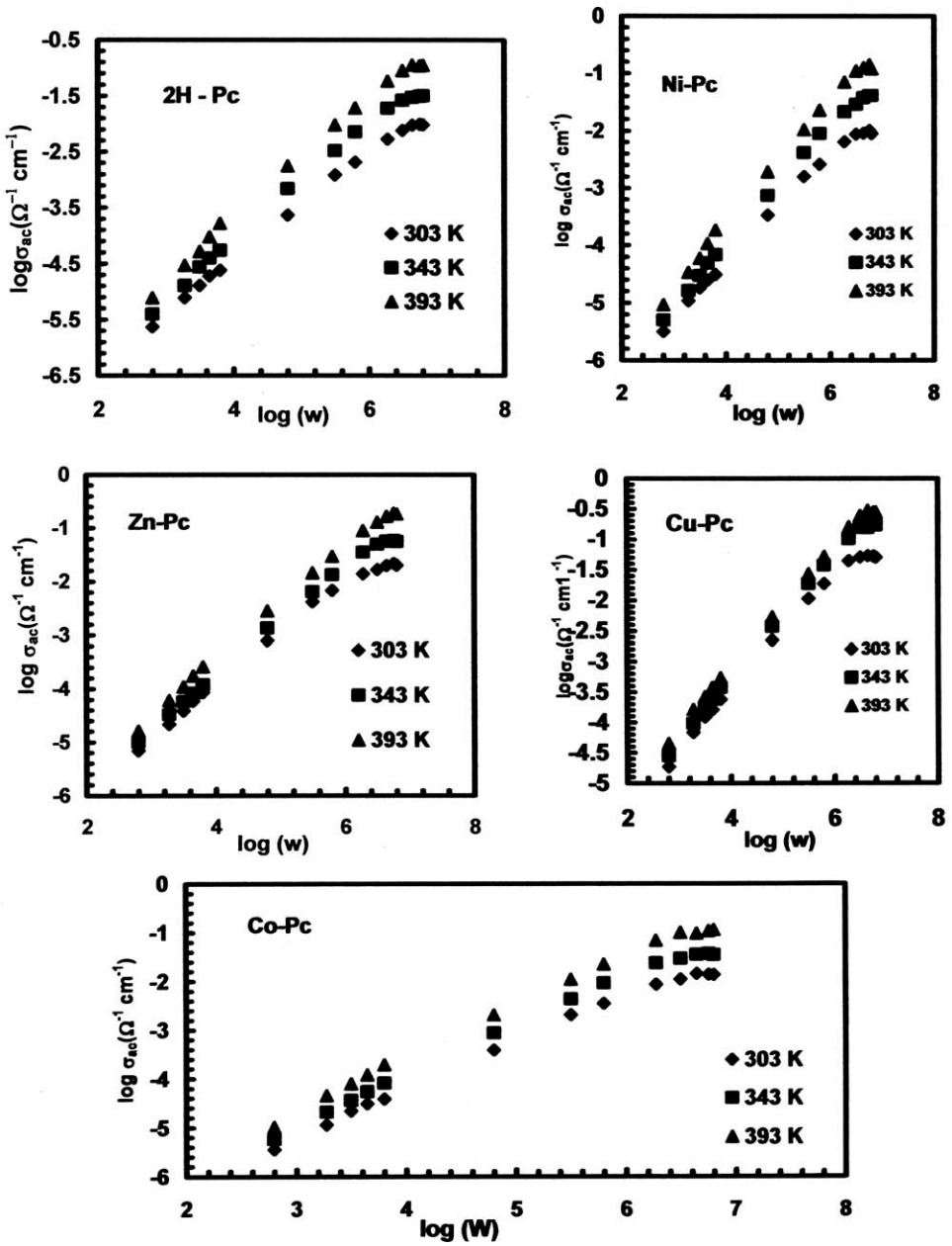

Figure 7 Dependence of ac conductivity on frequency for M-Pc at different temperatures.

temperature to a minimum value at a certain temperature, and then it continues to increase with increasing temperature. In the correlated barrier hopping model, the exponent s is given as:

$$S = 1 - \frac{6kT}{U_M - kT\ \ln(\frac{1}{\omega\tau_o})} \tag{6}$$

where U_M is the maximum barrier height at infinite separation, which is called the "polaron binding energy," i.e., the binding energy of the carrier in its localized sites and τ_o is a characteristic relaxation time which is in the order of an atom vibrational period $\tau_o = 10^{-13}$ sec.

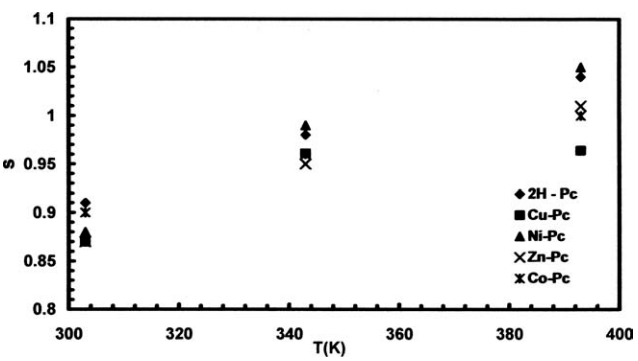

Figure 8 Thermal variation of the exponent s of M-Pc.

It is clear that (*s*) is both frequency and temperature dependent, besides its decrease from unity with increasing temperature. We see that among the above models, the NSPT is the most appropriate mechanism to explain the ac conduction behavior in the investigated samples. It is also important to mention that quantitative comparison between the different models is hampered by the distribution of relaxation times and energy barriers which could not be determined in this study.

CONCLUSIONS

A new full conjugated heterocyclic monomer can be synthesized in an efficient reaction between pyrenetetraone and diaminophthalonitrile. This monomer can be subjected to tetramerization affording new full conjugated metal free or M-Pc network polymers. The high molecular weight and solubility of these polymers make them easier for some applications.

Dielectric constant (ε'), dielectric loss tangent (tan δ), and ac conductivity (σ_{ac}) are found to be both frequency and temperature dependent through the studied ranges 10^2–10^6 Hz and 303–423 K, respectively. Both frequency and temperature dependence of the dielectric constant can be attributed to orientation and interfacial polarization, where the temperature dependence of dielectric loss tangent is associated with dielectric relaxation. The character of dependence of the exponent (s) on temperature has revealed that the NSPT model is the most dominate mechanism, which can contribute to the ac conduction behavior in the investigated samples.

References

1. McKeown, N. B. Phthalocyanine Materials: Synthesis, Structure and Function; Cambridge University Press: Cambridge, UK, 1998.
2. Milgrom, L. R. The Colours of Life: An Introduction to the Chemistry of Porphyrins and Related Compounds; Oxford University Press: New York, 1997.
3. Tang, C. W. Appl Phys Lett 1986, 48, 183.
4. Puigdollers, J.; Voz, C.; Fonrodona, M.; Cheylan, S.; Stella, M.; Andreu, J.; Vetter, M.; Alcubilla, R. J Non-Cryst Solids 2006, 352, 1778.
5. Nelson, J. The Physics of Solar Cells; Imperial College Press, UK, 2002; pp 17–39.
6. Imahori, H. J Phys Chem B 2004, 108, 6130.
7. Fujii, A.; Ohmori, Y.; Yoshino, K. IEEE Trans Electron Dev 1997, 44, 1204.
8. Liu, C. J.; Peng, C. H.; Ju, Y. H.; Hsieh, J. C. Sens Actuat B Chem 1998, 52, 564.
9. Wilson, A.; Wright, J. D. Mol Cryst Liq Cryst 1992, 211, 321.
10. Sharman, W. M.; van Lier, J. E. J. Porphyr Phthalocya 2000, 4, 441.
11. Leznoff, C. C. In: Phthalocyanines 2 Properties and Applications; Leznoff, C. C., Lever, A. B. P., Eds.; Willy-VCH, Germany, 1989; Vol. 1, pp 1–54.
12. Haas M., Liu S., Neels, A., Decurtins, S. Eur J Org Chem 2006, 24, 5467.
13. Singha, S. P.; Emina, S.; Loukanov, A. Adv Mat Lett 2010, 1, 148.
14. Faust, R.; Weber, C. J Org Chem 1999, 64, 2571.
15. Mitzel, F.; Gerald, S. F.; Beeby, A.; Faust, R. Chem Eur J 2003, 9, 1233.
16. Rusanova, J.; Pilkington, M.; Decurtins, S. Chem Commun 2002, 19, 2236.
17. Budd, P. M.; McKeown, N. B.; Fritsch, D. J Mater Chem 2005, 15, 1977.
18. Budd, P. M.; Ghanem, B.; Msayib, K.; McKeown, N. B.; Tattershall, C. J Mater Chem 2003, 13, 2721.
19. Kingsborough, R. P.; Swager, T. M. Angew Chem 2000, 16, 112.
20. Lidermann, K.; Lapcik, L., Jr. Carbohydr Polym 2000, 45, 369.
21. Yamato, T.; Fujumoto, M.; Miyazawa, A.; Matsuo, K. J. Chem Soc Perkin Trans 1997, 1, 1201.
22. Hu, J.; Zhang, D.; Harris, F.W. J Org Chem 2005, 70, 707.
23. Henari, F.; Davey, A.; Blau, W.; Haisch, P.; Hanack, M. J Porphyr Phthalocya 1999, 3, 331.
24. Jaung, J. Y.; Matsuoka, M.; Fukunishi, K. Synthesis 1998, 9, 1347.
25. Puigdollers, J.; Voz, C.; Fonrodona, M.; Cheylan, S.; Stella, M.; Andreu, J.; Vetter, M.; Alcubilla, R. J Non Cryst Solids 2006, 352, 1778.
26. Wizel, S.; Margel, S.; Gedanken, A.; Rojas, T. C.; Ferna'ndez, A.; Prozorov, R. J Mater Res 1999, 14, 3913.
27. Chen, Q.; Gu, D.; Gan, F. Physica B 1995, 212, 189.
28. Moynihan, C. T.; Boesch, L. B.; Laberge, N. L. Phys Chem Glass 1973, 14, 122.
29. Macedo, P. B.; Moynihan, C. T.; Base, R. Phys Chem Glass 1972, 13, 171.
30. Kurien, S.; Mathew, J.; Sebastian, S.; Potty, S. N.; George, K. C. Mater Chem Phys 2006, 98, 470.
31. Bunget, I.; Popescu, M. Solid Dielectric; Elsevier: New York, 1984.
32. Anantha, P. S.; Harihanan, K.; Mater Sci Eng B 2005, 121, 12.
33. Zakowski, P. W.; Kantorow, S. B.; Maczka, D.; Stelakh, V. F. Phys Stat Sol (a) 1989, 112, 695.
34. Vasudevan, A.; Carin, S.; Melloch, M. R.; Harmon, E. S. Appl Phys Lett 1998, 73, 671.
35. Lin, H. M.; chen, Y. F.; Shen, J. L.; Chou, C. W. Appl Phys Lett 2001, 78, 1909.
36. Abd El-kader, F. H.; Osman, W. H.; Mahmoud, K. H., Basha, M. A. F. Phys B 2008, 403, 3473.
37. Mahmoud, K. H.; Abdel-Rahim, F. M.; Atef, K.; Saddeek, Y. B. Curr Appl Phys 2011, 11, 55.
38. Lannfredi, S.; Saia, P. S.; Lebullenger, R.; Hernandes, A. C. Solid State Ionics 2002, 146, 3291.
39. Mott, N. F.; Davis, E. A. Electronic Processes in Non-Crystalline Materials, 2nd ed.; Clarendon: Oxford, 1979.
40. Ghosh, A. Phys Rev B 1990, 41, 1479.
41. Long, R. Adv Phys 1982, 31, 553.
42. Elliot, R. Adv Phys 1978, 36, 135.